JGR Atmospheres

RESEARCH ARTICLE
10.1029/2022JD037199

Influences of Antarctic Ozone Depletion on Southern Ocean Aerosols

Yusuf. A. Bhatti[1], **Laura. E. Revell**[1], **and Adrian. J. McDonald**[1,2]

[1]School of Physical and Chemical Sciences, University of Canterbury, Christchurch, New Zealand, [2]Gateway Antarctica, University of Canterbury, Christchurch, New Zealand

Key Points:

- Wind-driven Southern Ocean aerosol fluxes are influenced by the ozone hole during austral summer
- Austral summer sea spray aerosol increased by 9.7% and dimethyl sulfide increased by 3% around 60°S between 1940 and 2014
- Indirect influences of ozone losses mean Southern Ocean aerosols cannot be considered to be representative of pristine conditions

Supporting Information:

Supporting Information may be found in the online version of this article.

Correspondence to:

Y. A. Bhatti,
yusuf.bhatti@pg.canterbury.ac.nz

Citation:

Bhatti, Y. A., Revell, L. E., & McDonald, A. J. (2022). Influences of Antarctic ozone depletion on Southern Ocean aerosols. *Journal of Geophysical Research: Atmospheres*, *127*, e2022JD037199. https://doi.org/10.1029/2022JD037199

Received 1 JUN 2022
Accepted 4 SEP 2022

Abstract The Southern Ocean is often identified as a pristine aerosol environment, being distant from anthropogenic sources. We investigate anomalies in aerosol loading over the Southern Ocean due to stratospheric ozone depletion in historical simulations performed for the sixth Coupled Model Intercomparison Project. We explore direct influences of ozone depletion on aerosols via enhanced ultraviolet-induced production of oceanic dimethyl sulfide (DMS), and indirect influences via changes in the Southern Hemisphere westerly jet, which impacts wind-driven aerosol fluxes. We identify wind as the key driver of change for austral summertime aerosol, leading to increases in aerosol optical depth of up to 24% compared with the pre–ozone hole era. In contrast to previous studies, direct impacts on aerosol from ozone depletion and enhanced ultraviolet fluxes are less obvious. Our results show that the Southern Ocean summertime aerosol environment cannot be considered to be representative of pre–ozone hole conditions because stratospheric ozone depletion has indirectly increased marine aerosol fluxes.

Plain Language Summary Studies performed in the 2000s suggested that the Antarctic ozone hole would lead to increased marine biogeochemical activity, increasing the concentration of phytoplankton-produced dimethyl sulfide, and therefore sulfate aerosol. Our analysis shows that this feedback is not significant in a range of state-of-the-art Earth System Models. However, because the ozone hole influences the summertime near-surface westerly jet, the impact of wind-driven aerosol formation has increased by up to 24% over the Southern Ocean since stratospheric ozone depletion began. The Southern Ocean is typically considered a pristine environment for aerosols, especially during summer months. Our results imply that, far from being pristine, the Southern Ocean has experienced significant human-induced change ever since Antarctic ozone depletion began.

1. Introduction

The atmosphere above the Southern Ocean has often been described as a pristine environment for studying aerosols due to its remote location, meaning that anthropogenic influences are minor (Hamilton et al., 2014; McCoy et al., 2020). Aerosols over the Southern Ocean derive from natural sources: sea spray aerosol (SSA) is injected into the atmosphere via the breaking of waves and air bubbles bursting, forming the main source of primary aerosol. Secondary aerosols such as sulfate aerosol originate from dimethyl sulfide (DMS) oxidation, with the DMS originating from biological activity in the surface ocean. SSA and sulfate aerosols are important in several ways, for example, they are the dominant contributors to cloud condensation nuclei over the Southern Ocean (Humphries et al., 2021). Aerosol loading over the Southern Ocean maximizes annually during summertime, which can be attributed to enhanced sulfate aerosol production linked to variations in DMS production. The rate of DMS production is linked to marine biology, which is in turn influenced by seasonal changes in ultraviolet (UV) light (e.g., Fossum et al., 2018; Korhonen et al., 2008; Vallina et al., 2006).

Over the past few decades, stratospheric ozone depletion has resulted in numerous changes in Southern Hemisphere spring and summer surface climate (e.g., Arrigo, 1994; Farman et al., 1985; Gonzalez et al., 2014; Son et al., 2018; Thompson et al., 2011). In particular, fluxes of UV light at high latitudes have changed in recent decades owing to springtime ozone depletion over Antarctica. Enhanced surface UV-B fluxes at southern high latitudes have impacted the biosphere, for example, the mortality of krill and other marine species has increased (Llabrés et al., 2013; Peng et al., 2017). Furthermore, ozone depletion has cooled the stratosphere, leading to an indirect intensification and poleward shift in the tropospheric westerly jet by 15%–20% (Son et al., 2018; Swart & Fyfe, 2012; Thompson & Solomon, 2002; Thompson et al., 2011). The greatest changes to tropospheric

Table 1
Sixth Coupled Model Intercomparison Project Models Used in This Study

Model (ensembles)	Reference	U_{10}	SSA	AOD_{550}	DMS	Oceanic DMS
UKESM1 (8)	Tang et al. (2019)	✓	✓	✓	✓	✓
BCC-ESM1 (3)	Wu et al. (2018)	✓	✓	✓	✓	
GFDL-CM4 (1)	Krasting et al. (2018)	✓	✓	✓	✓	
HadGEM3-GC3.1-LL (4)	Ridley et al. (2019)	✓	✓	✓	✓	
MRI-ESM2-0 (5)	Yukimoto et al. (2019)	✓	✓	✓	✓	
NorESM2-LM (3)	Seland et al. (2019)	✓	✓	✓	✓	✓
GFDL-ESM4 (1)	Krasting et al. (2018)	✓	✓	✓	✓	
MPI-ESM-1-2-HAM (3)	Neubauer et al. (2019)	✓	✓	✓	✓	
MIROC-ES2L (27)	Tatebe and Watanabe (2018)	✓			✓	✓

Note. U_{10}, sea spray aerosol (SSA) and AOD_{550} represent wind speeds at 10 m above sea level, sea-spray aerosol and aerosol optical depth at 550 nm respectively. Surface level oceanic and atmospheric dimethyl sulfide (DMS) is analyzed here. The number in brackets depicts the number of ensemble members used from each respective model.

winds are seen in austral summer, when Southern Ocean biological productivity is at its greatest (Gillett & Thompson, 2003; Ivy et al., 2016; Orr et al., 2012; Swart et al., 2015; Thompson & Solomon, 2002).

Higher wind speeds result in both a higher sea-to-air flux of DMS (e.g., Bell et al., 2013, 2015; Ho et al., 2006; Liss & Merlivat, 1986; Yang et al., 2011), and increased production of SSA (Gong, 2003; Grythe et al., 2014; Hartery et al., 2020; Jaeglé et al., 2011; Korhonen et al., 2010; L. E. Revell et al., 2019, 2021). Therefore, changes in the westerly jet in response to stratospheric ozone depletion might be expected to increase sulfate aerosol burden and SSA. Since measurements of Southern Ocean aerosols and their precursors are spatially and temporally sparse, we investigate the sensitivity of Southern Ocean marine aerosol abundances to Antarctic ozone depletion using Earth system model simulations performed for the sixth Coupled Model Intercomparison Project (CMIP6) (Eyring et al., 2016).

We investigate the response of Southern Ocean aerosol loading to direct influences of ozone depletion (related to UV-induced changes in ocean biogeochemistry and DMS production; Section 3.1) and indirect influences of ozone depletion (via the poleward shift and strengthening of the westerly winds over the Southern Ocean; Section 3.2).

2. Methods

2.1. Model Description

We analyzed historical ("hist") simulations performed for the Sixth Coupled Model Intercomparison Project (CMIP6; Eyring et al. (2016)). The nine models used in this paper are outlined in Table 1.

Our seasons of interest are austral spring and summer. Spring is when the greatest depletion of total column ozone occurs (e.g., Solomon, 1999), which is the focal point of the direct influence on the atmosphere (Section 3.2). Summer is when the greatest perturbations in surface climate arising from the ozone hole are experienced, primarily via the strengthening and poleward movement of the westerly jet (e.g., Thompson & Solomon, 2002; Thompson et al., 2011) (Section 3.1). The models used for the indirect atmospheric perturbation analysis have a median total column ozone bias of ±0.86 DU relative to observations (Keeble et al., 2021), and a westerly jet speed bias of +0.34 m s^{-1} relative to the ERA5 reanalysis (T. Bracegirdle, Holmes, et al., 2020). Improvements in Southern Ocean winds from previous CMIP5 models mostly occur during summer and spring, with large improvements to the westerly jet index (T. Bracegirdle, Holmes, et al., 2020).

Three of the models (UKESM1, MIROC6 and NorESM2) calculate oceanic DMS online via an ocean biogeochemistry scheme. Ocean biogeochemistry from the UKESM1 and MIROC6 models is calculated via empirical parameterizations, whereas NorESM2 uses a prognostic approach. Bock et al. (2021) comprehensively evaluate oceanic DMS in these models.

For the transfer of oceanic DMS into the atmosphere, all models used in this study have a sea-to-air flux parameterization dependent on wind speed (Table S1 in Supporting Information S1). All parameterizations have a similar high wind speed dependency at 10 m above sea level (U_{10}; Liss and Merlivat (1986), Wanninkhof (1992), Nightingale et al. (2000), Wanninkhof (2014)). SSA production in all models is dependent on wind speed and sometimes sea-surface temperature (Table S2 in Supporting Information S1; Gong (2003), Mahowald et al. (2006), Jaeglé et al. (2011), Long et al. (2011), Sofiev et al. (2011), Salter et al. (2015)).

Gong (2003) is the most commonly used parameterization (3 models) and represents SSA productions only as a function of wind speed. The other six models analyzed in this study (GFDL-CM4, GFDL-ESM4, NorESM2-LM, MPI-ESM-1-2-HAM, and MIROC-ES2L) also include a sea-surface temperature dependency. L. E. Revell et al. (2021) showed that replacing the Gong (2003) SSA parameterization with the Jaeglé et al. (2011) parameterization decreased AOD biases relative to MODIS observations over the Southern Ocean.

To assess wind variability at sub-daily temporal resolution (which is unavailable from the CMIP6 data set) and its influence on aerosol production, 3 hourly 10 m wind speeds are analyzed from the ERA5 reanalysis (Hersbach et al., 2020). This is discussed in greater detail in Section 3.1.

2.2. Simulations

To assess atmospheric changes in response to ozone depletion, we derived a multi-model median climatology for the period prior to the onset of stratospheric ozone depletion (1940–1960), as a baseline. Our present-day period is a climatology of 1995–2014 commonly used across the literature (e.g., T. Bracegirdle, Holmes, et al., 2020). The calculated atmospheric changes (Δ) are the difference between the present-day (1995–2014) and past (1940–1960) climatology.

Atmospheric DMS concentrations from the lowermost model level (20 m above sea level) are analyzed, along with near-surface westerly wind speeds at 10 m above sea level. Aerosol optical depth (AOD) is analyzed at 550 nm, as provided to CMIP6 (Table 1). We examine two potential drivers of changes in aerosol loading resulting from stratospheric ozone depletion across summer and spring, discussed in Sections 3.1 and 3.2, respectively. Sea ice extent is defined here as grid cells with a concentration $\geq$15%, which is the traditional definition outlined by Cavalieri et al. (1991). Model data within the sea ice extent was removed for our calculations. Statistical significance was calculated using the Student's *t*-test at the 95% level of confidence in the present-day period relative to the baseline period.

3. Results and Discussion

3.1. Indirect Influences of Stratospheric Ozone Depletion on Aerosol During Austral Summer

Because ozone absorption of UV-B radiation heats the stratosphere, springtime ozone destruction causes the stratosphere to cool. The resulting cooling influences the Southern Hemisphere stratospheric westerly jet by changing the thermal wind balance, with a lagged shift in the tropospheric jet, meaning that the influence of the ozone hole on tropospheric winds is observed in austral summer (Son et al., 2018; Thompson & Solomon, 2002). The lower tropospheric westerly jet has a significant influence on Southern Hemisphere climate, with changes in the jet strength and position leading to changes in air temperature, precipitation and the location and intensity of the storm tracks (Son et al., 2009; Thompson et al., 2011). From the mid-1980s onwards, the westerly jet strengthened and shifted poleward. CMIP6 simulations show that near-surface (10 m) westerly winds weakened by approximately 0.34 m s^{-1} at 40°S, and strengthened by 1.14 m s^{-1}, representative of this poleward shift (Figures 1a, and 2a), consistent with observations (Goyal et al., 2021; T. J. Bracegirdle, Holmes, et al., 2020).

As wind is a key driver of marine aerosol emissions, we assess changes in DMS, SSA and AOD (Figures 1b–1d) in regions where winds have changed in the summer. Summertime SSA fluxes (Figures 1c, 2c,) increased by 9.7% around 60°S, but decreased by 2.6% at 40°S, coinciding with similarly signed latitudinal changes in wind speed. SSA at 60°S increased by up to 29% in places. Overall, SSA fluxes across the entire Southern Ocean (40–60°S) increased by approximately 3.2%. We therefore see slight reductions in AOD at lower latitudes (Figures 1d and 2d), but enhanced aerosol loading at higher latitudes driven primarily by increased SSA fluxes (Figures 1c and 2c).

Similar to SSA, changes in Southern Ocean atmospheric DMS (Figure 1b) can be linked to anomalies in wind speed through the late 20th and early 21st century due to the DMS sea-to-air flux and its dependency on wind

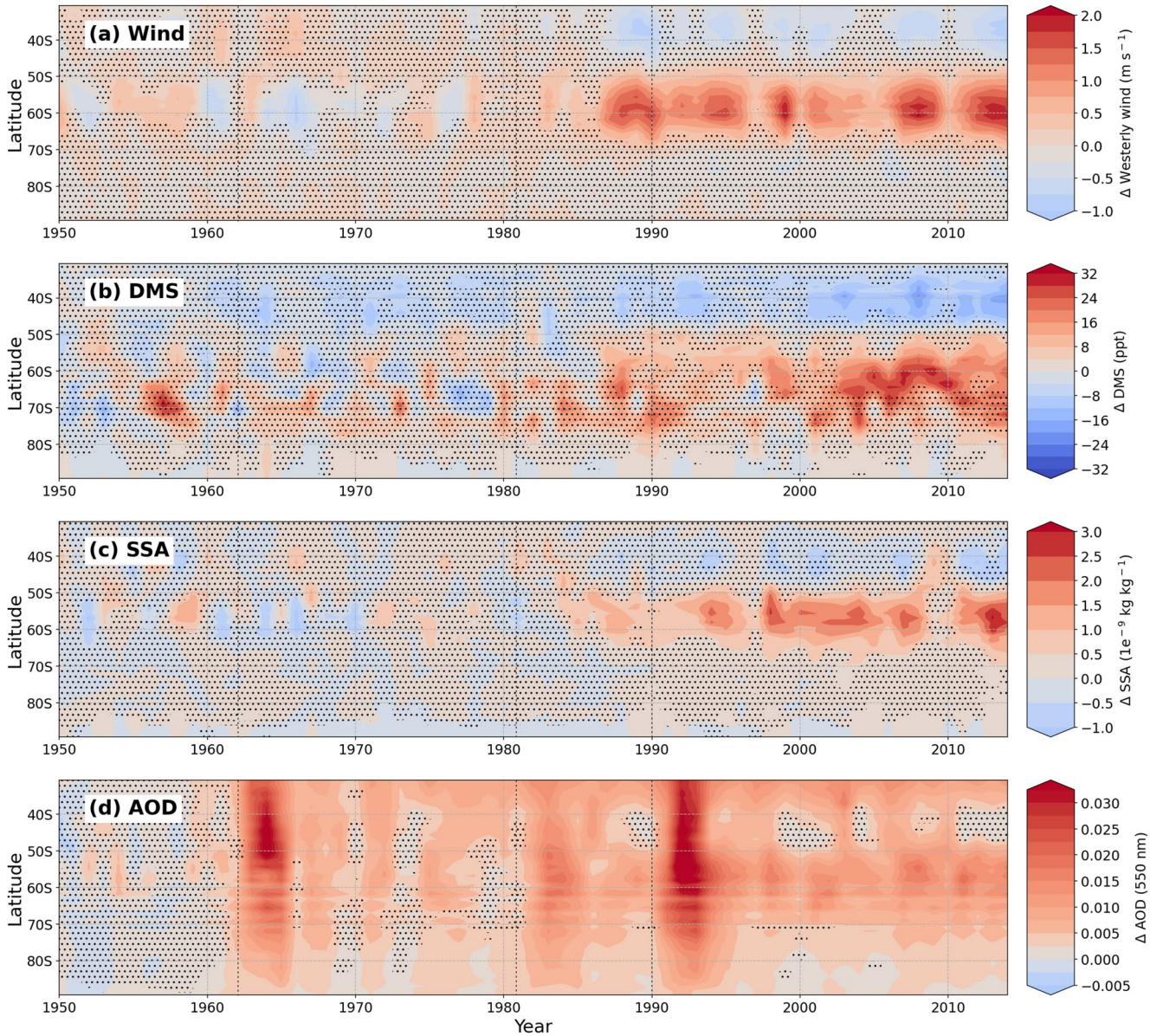

Figure 1. Sixth Coupled Model Intercomparison Project multi-model median (a) change in Southern Ocean near-surface westerly winds in December–February (DJF) relative to the 1940–1960 DJF climatology. (b–d) As for (a), but showing atmospheric dimethyl sulfide (DMS), sea spray aerosol (SSA) and Aerosol optical depth (AOD), respectively. Hatching indicates where the differences are not statistically significant (95% level of confidence, Student's *t*-test). Vertical dashed lines at 1963, 1982 and 1991 represent the volcanic eruptions of Mt. Agung, El Chichón and Pinatubo, respectively.

speed (Table S1 in Supporting Information S1). Between 1940–1960 and 1995–2014, near-surface atmospheric DMS increased on average by around 3% (8.7 ppt) at 60°S, and increased by more than 15% (40 ppt) in places around the 60°S latitude circle during DJF (Figures 1b, 2b, and 2e). Large decreases in DMS of up to 24% (16 ppt) are simulated at 40°S. Overall, DMS increased by 0.82% over the Southern Ocean.

Sea spray aerosol is the dominant contributor to aerosol mass over the Southern Ocean due to its emission into the larger aerosol modes, the accumulation mode (50–500 nm) and coarse mode (>500 nm) (Korhonen et al., 2008; Mulcahy et al., 2020). As a result of this large particle size distribution, SSA dominates the proportions which make up AOD. Summertime AOD over the Southern Ocean increased by 5.6% in the CMIP6 models, but with averages of +11.3% around 60°S. This latitude where regional changes in wind speeds have maximized coincides with the maximum localized AOD increase-up to 23.9%, or 0.026 (dimensionless) at 550 nm (Figure 1d).

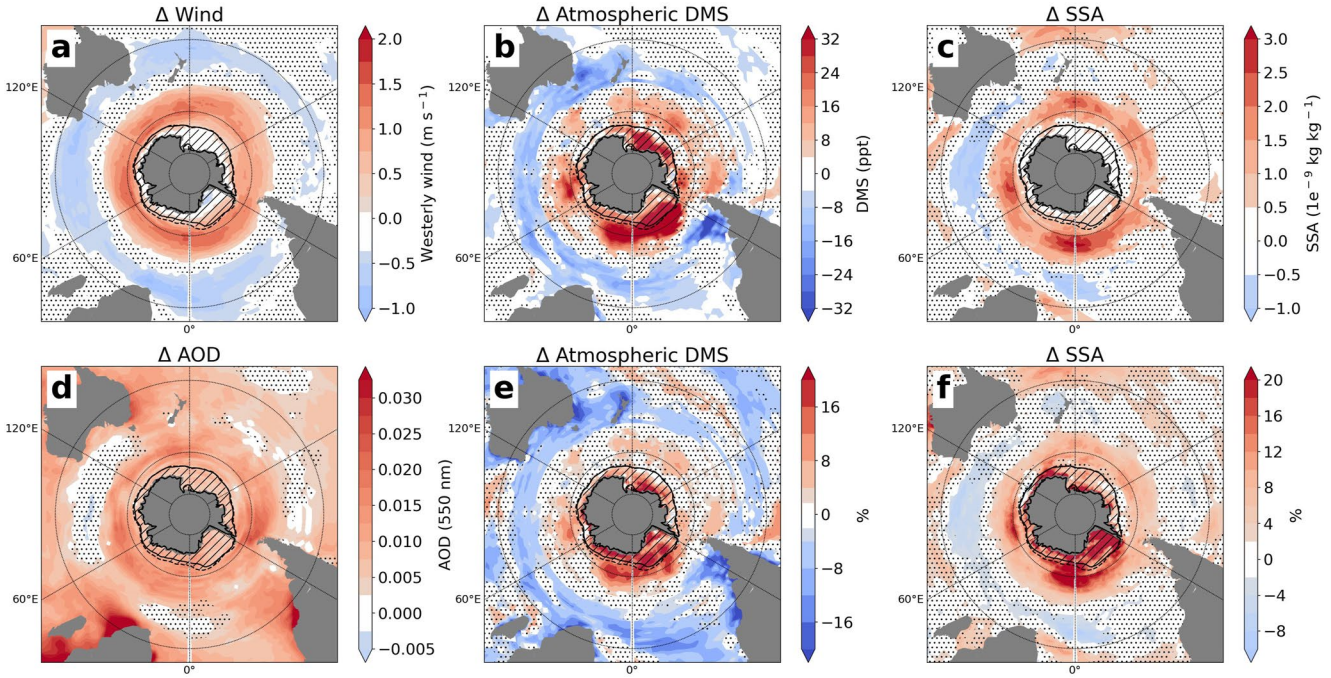

Figure 2. Sixth Coupled Model Intercomparison Project multi-model median (a) Change in Southern Ocean near-surface westerly winds in December–February in 1995–2014 relative to the 1940–1960 mean. The black solid line represents the 1995–2014 mean sea ice extent, and hatching shows the 1940–1960 sea ice extent, defined as grid cells with a sea ice concentration ≥15%. (b–f) As for (a), but showing (b) absolute changes in near-surface atmospheric dimethyl sulfide (DMS) concentrations, (c) absolute changes in near-surface sea spray aerosol (SSA) concentrations, (d) absolute changes in aerosol optical depth at 550 nm, (e) relative changes in near-surface atmospheric DMS concentrations, (f) relative changes in near-surface SSA concentrations. Hatching indicates where the differences are not statistically significant (95% level of confidence, Student's *t*-test).

Figure 3 presents time series of mean and median zonal wind, AOD, SSA and DMS over the Southern Ocean simulated by the CMIP6 models. Although there is inter-model variability, the mean and median trends are consistent with what would be expected for the Southern Ocean. Both the mean and median show the variability between individual models, with the median giving a representation of CMIP6 without including the outliers. Individual models are shown in Figure S1 in Supporting Information S1. The indirect influence of stratospheric ozone-induced changes on the westerly winds, and therefore Southern Ocean aerosol loading, have resulted in significant spatial changes. Recent observations show that strengthening of the westerly jet has slowed down and even paused (Banerjee et al., 2020), leading to the question of whether changes in wind-driven marine aerosol fluxes over the high latitude Southern Ocean (~60°S) have yet to reach their maximum. Given westerly jet projections in the CMIP6 models (Goyal et al., 2021; T. J. Bracegirdle, Holmes, et al., 2020), under the greenhouse gas emissions scenario Shared Socioeconomic Pathway (SSP) 245 (Meinshausen et al., 2020), we would expect to see a plateau in aerosol loading throughout the 21st century, given that the influence of ozone recovery counteracts the effects of greenhouse gas forcing in this scenario. Under the high emissions scenario SSP585, the westerly jet is projected to strengthen and move poleward through the 21st century. We would therefore expect to see larger increases in aerosol loading at higher latitudes, further perturbing Southern Ocean climate. Greenhouse gas induced warming may therefore lead to even greater wind-driven aerosol increases in the future. To some extent, direct aerosol-radiation and aerosol-cloud interactions would offset increases in greenhouse gas radiative forcing (L. Revell et al., 2022). Furthermore, very large aerosol loading over the Southern Ocean could cause the jet to weaken and move equatorward (L. E. Revell et al., 2021).

Radiative forcing changes over the Southern Ocean presents similar spatial patterns to the changes shown in wind, with an increase of 1.27 W m^{-2} at 60°S and decreases by 0.64 W m^{-2} at 40 °S (not shown). Southern Ocean cloud-radiation interactions has much more profound influence (around 10 times greater magnitudes of change) than the aerosol-radiation interaction on the all-sky radiative forcing. Large shifts in radiation have occurred due to the shifts in natural aerosol, coinciding with Carslaw et al. (2013) on the importance for understanding pristine environments, like the Southern Ocean.

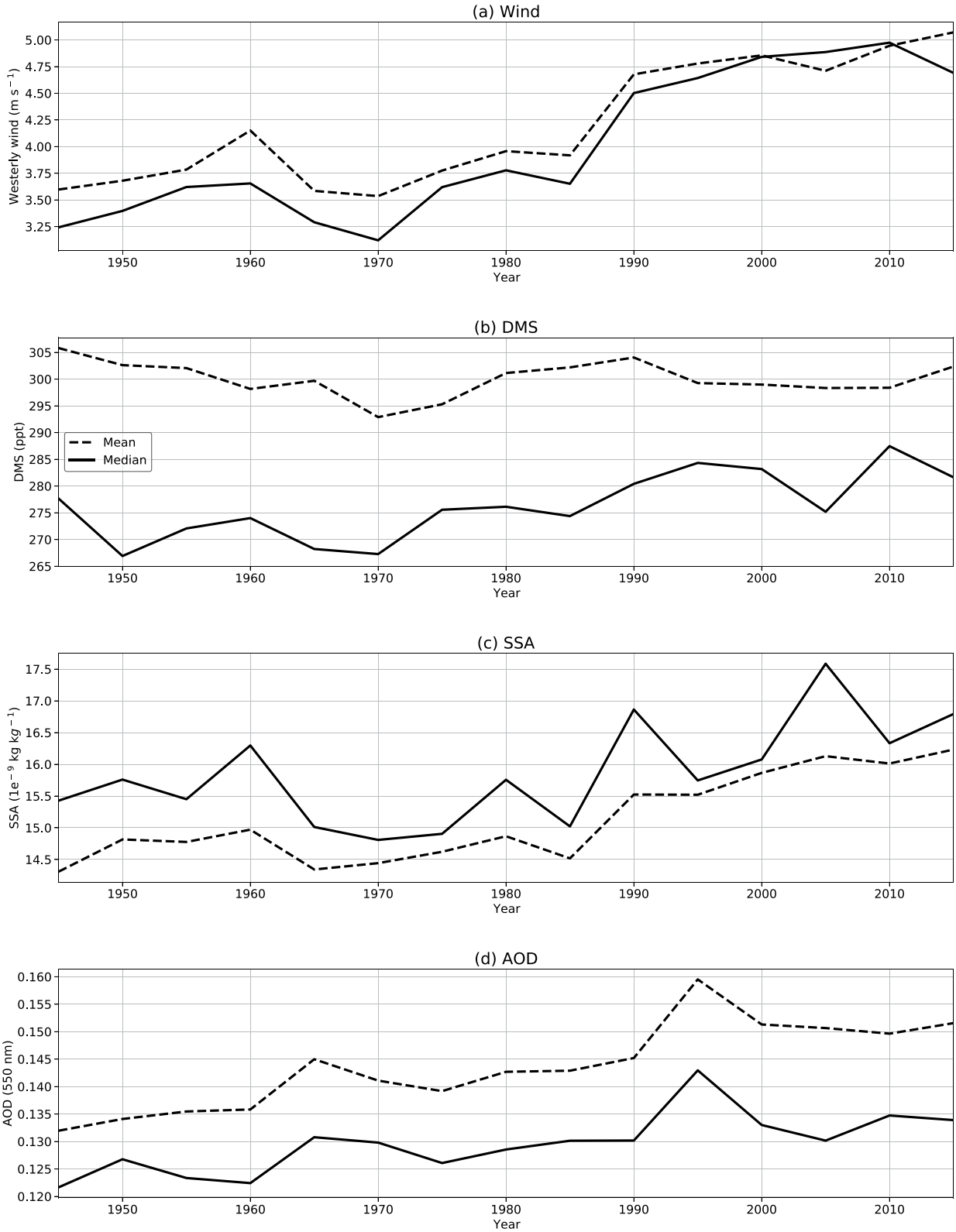

Figure 3. Temporal evolution over approximately 60°S of December–February (a) near-surface westerly winds, (b) atmospheric dimethyl sulfide (DMS), (c) Sea-salt aerosol and (d) aerosol optical depth at 550 nm. The 5 year rolling median and mean values are shown by the solid black and dashed black lines, respectively. Individual models are labeled in Figure S1 in Supporting Information S1.

Sea ice change in CMIP6 simulations in DJF have had some impacts on aerosol loading. For example, the largest area of sea ice change, east of the Antarctic Peninsula, correlates strongly with SSA increases ($r^2 = 0.91$; Figure S2f in Supporting Information S1). However, the limited amount of sea ice in summer means that any changes connected to sea ice change in this season are limited.

Biases in CMIP6 models may cause further perturbation on climatic changes within this study. CMIP6 simulations have been extensively validated against measurements (e.g., Eyring et al., 2016; Goyal et al., 2021; Keeble et al., 2021; Séférian et al., 2020; Schuddeboom & McDonald, 2021; T. Bracegirdle, Holmes, et al., 2020). Although the averaged CMIP6 simulations agree well with total column ozone measurements, large inter-model variability is present within the CMIP6 ensemble (Keeble et al., 2021). Biases in total column ozone can propagate to biases in the strength and southward progression of the westerly jet (Lin et al., 2017; L. Revell et al., 2022; Son et al., 2018).

Korhonen et al. (2010) identified that increased SSA fluxes, CCN concentrations and cloud radiative forcing due to increases in Southern Ocean westerly wind speeds may more than double the negative radiative forcing from stratospheric ozone loss and represent an important climate feedback. However, model validation and the sparsity of observational measurements in this region meant that Korhonen et al. (2010) had difficulties distinguishing between the effects of perturbations from westerly wind shifts and model bias. DMS sea-to-air parameterizations pose issues with higher levels of uncertainty when wind speeds exceed 13 m s^{-1} (Blomquist et al., 2017; Krall et al., 2019), particularly using the Liss and Merlivat (1986) parameterization which is used in multiple CMIP6 models, as this is a key threshold (Equation S1 in Supporting Information S1). Blomquist et al. (2017) shows K (transfer velocity) for DMS to have a relatively small uncertainty when $U_{10} \leq$ 12–13 m s^{-1}, but can reach as high as 30%–40% when U_{10} is 15 m s^{-1}.

T. Bracegirdle, Holmes, et al., 2020 identified the positioning of the westerly jet at 50.92°S, with a climatological wind speed at 12.81 m s^{-1}. The CMIP6 models used in this study have wind speed biases as described by T. Bracegirdle, Holmes, et al., 2020, but are generally small. We therefore use ERA5 reanalysis hourly surface wind speeds between 1995 and 2014 to derive representative probabilities of speeds above 13 m s^{-1} over the latitudinal bands of interest used in this study because of a lack of relevant CMIP6 data (not shown). In particular, the occurrence of wind speeds reaching above 13 m s^{-1} at 40°S is 2% of the time in ERA5, while at 60°S these winds occur 5% of the time. Across the entire Southern Ocean, the frequency of wind speeds ≥13 m s^{-1} is 6%, with the most frequent occurrence around 51°S. For wind speeds ≥15 m s^{-1} the frequency of occurrence is less than 2% of the time for both latitudinal bands. Within CMIP6, BCC-ESM1 produces the largest DMS and AOD (Figures S2b and S2d in Supporting Information S1) partly as a response to the high biased wind speeds simulated. BCC-ESM1 is a statistical outlier (≥95th percentile) for DMS and AOD across the CMIP6 data set, contain the highest westerly jet speed bias (+2.13 m s^{-1}), simulating a climatological westerly jet of 14.94 m s^{-1}. Higher BCC-ESM1 wind speeds therefore occur much more frequently than expected from ERA5. As BCC-ESM1 incorporates the Liss and Merlivat (1986) sea-to-air parameterization (Table S1 in Supporting Information S1), much higher volumes of atmospheric DMS would be produced at these higher wind speeds, corresponding to higher uncertainty levels (13–15 m s^{-1}). Therefore we suggest that based on the ERA5 representation of diurnal wind patterns and the similarity between the median wind speed of ERA5 and the CMIP6 models used in this study that the CMIP6 models, with exception of BCC-ESM1, are likely not strongly impacted by uncertainty in aerosol loading associated with very high wind speeds.

3.2. Influences of Ozone Depletion on Aerosols in Austral Spring

3.2.1. Direct Influences on Aerosol

Along with changes in wind speed, oceanic and atmospheric DMS are also affected by changes in incoming solar radiation which influences ocean biogeochemistry. Figure 4a shows the springtime depletion of total column ozone by approximately 140–158 DU over the Antarctic. Top of the atmosphere all-sky and clear-sky radiative forcing increased by 2.8 W m^{-2} and 2.9 W m^{-2} respectively, over continental Antarctica and the surrounding ocean, which agrees with Chiodo et al. (2017) suggesting less shortwave radiation has been absorbed by ozone. As downward shortwave radiation increases within the ozone hole area, we might expect to see decreases in oceanic DMS production as suggested by Yool et al. (2013, 2020).

Despite previous studies suggesting that enhanced UV-B fluxes due to ozone depletion would reduce marine DMS production (e.g., Arrigo, 1994; Erickson III et al., 2000; Larsen, 2005; Smith et al., 1992; Zepp et al., 2007),

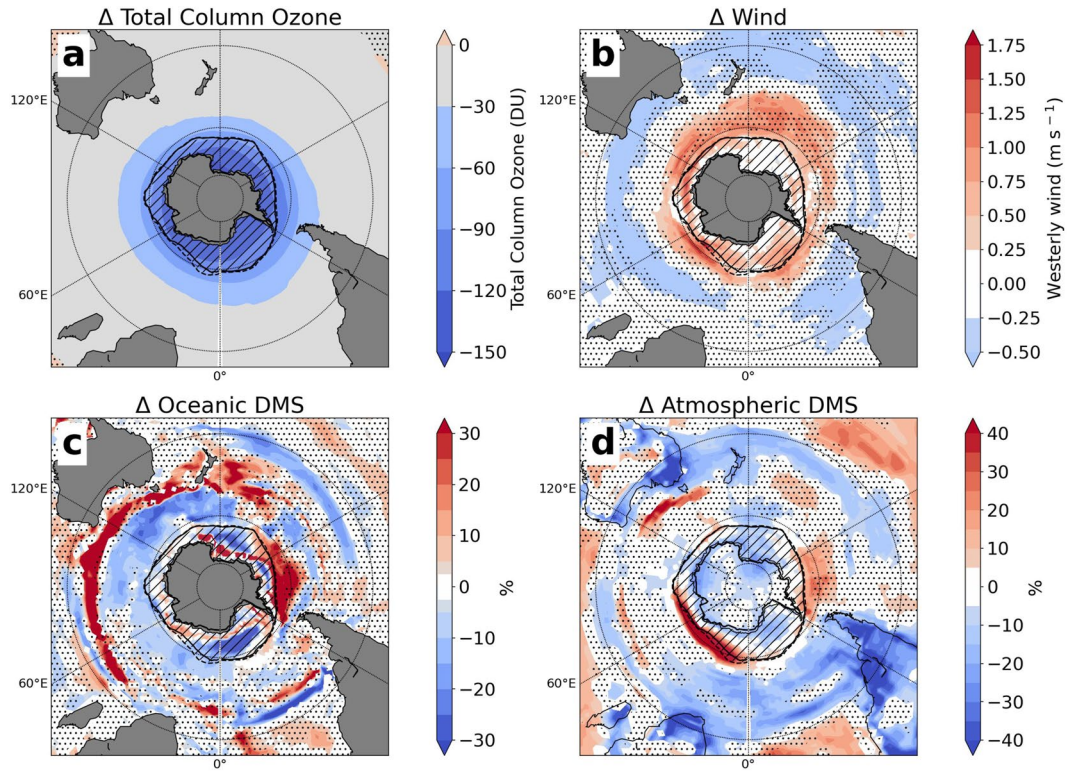

Figure 4. (a) Change in total column ozone in SON in 1995–2014 relative to the 1940–1960 climatology. The black solid line represents the 1995–2014 mean sea ice extent, and hatching shows the 1940–1960 sea ice extent. (b–d) As for (a), but showing (b) changes in near-surface (10 m) westerly winds, (c) relative changes in oceanic dimethyl sulfide (DMS) concentrations, (d) relative changes in near-surface (20 m) atmospheric DMS concentrations. Hatching indicates where the differences are not statistically significant (95% level of confidence, Student's *t*-test).

models shows small changes in springtime oceanic DMS (Figure 4c). The largest changes in oceanic DMS in the Southern Ocean occur around 40°S where values range from +1.83 nM to −1.1 nM (Figure 4c). Large proportions of these changes coincide with wind perturbations (Figure 4b). Statistically significant increases of up to 88% in the oceanic DMS relative to the 1940–1960 climatology are simulated toward the higher latitudes, just outside the sea ice zone, west of the Antarctic Peninsula. However, this cannot be clearly attributed to shortwave radiation change given the approximately zonally symmetric distribution of stratospheric ozone depletion (Figure 4a). Over continental Antarctica, model output suggests atmospheric DMS has decreased by 0.5 ppt or 30% relative to the 1940–1960 climatology (Figure 4d in Supporting Information S1), with the inter-model variability ranging between −70% (0.26 ppt; NorESM2-LM) and −8% (0.5 ppt; MIROC-ES2L) (Figure S3–S5 in Supporting Information S1). A. E. Jones and Wolff (2003) suggest the South Pole troposphere is highly oxidizing due to the ozone hole, which may have played a role in the removal of DMS. The uncertainty in aqueous-phase chemical reactions for DMS oxidation cascades to uncertainty in the cloud droplet number concentration (CDNC) over oceanic regions, such as the Southern Ocean (Veres et al., 2020). Additionally, climate models contain simplistic DMS oxidation chemistry schemes hindering the full real-world process of DMS to aerosol formation (Hoffmann et al., 2016; L. E. Revell et al., 2019). Future work will focus on introducing comprehensive chemistry schemes. The strong increase in atmospheric DMS (Figure 4d) which is bounded by the sea ice zone likely reflects sea ice melt, prominent within just UKESM1 (Figure S3 in Supporting Information S1), with the role of sea ice discussed in Section 3.2.2.

All the models used for understanding the direct influences of ozone depletion on oceanic DMS disagree on how the climatology of the Southern Ocean has changed, consistent with Bock et al. (2021). Using the multi-model average gives the best representation of the climatology relative to observations as Bock et al. (2021) finds it has the lowest root mean square error and highest pattern correlation when compared with observational measurements. Bock et al. (2021) noted that NorESM2-LM represents oceanic DMS better than the other models

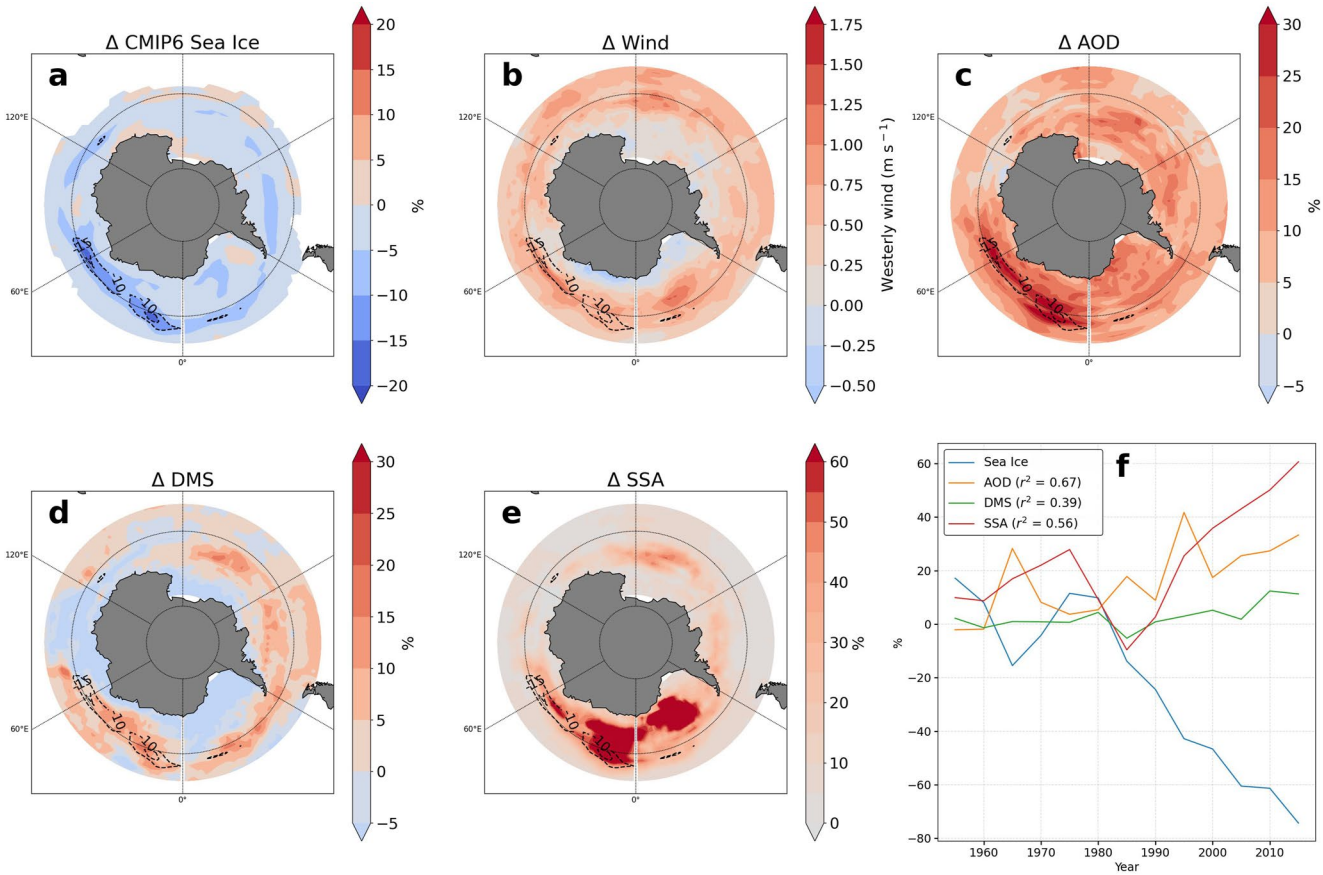

Figure 5. (a) Change in Southern Ocean sea ice extent during SON in 1995–2014 relative to the 1940–1960 climatology. Contours show area of sea ice melt ≥10%. (b) As for (a), but showing changes in near-surface (10 m) westerly winds, (c) as for (a), but showing relative changes in aerosol optical depth, (d) As for (a), but showing relative changes in atmospheric dimethyl sulfide (DMS), (e) as for (a), but showing relative changes to sea-salt aerosol. (f) Percent change in the 5 year rolling mean of sea ice, Aerosol optical depth (AOD), dimethyl sulfide (DMS) and sea spray aerosol (SSA) relative to 1940–1960, averaged within the sea ice melt contours shown in (a-e). The r^2 values for AOD, DMS and SSA within the contours of sea ice loss are shown.

when compared with observational data, but falls shorts of the multi-model average (Figure S4 in Supporting Information S1).

3.2.2. Indirect Influences on Aerosol

The westerly jet and SAM have changed significantly during summer, but smaller changes are also observed during spring with the westerly jet shifting poleward (Figure 4b). These changes would be expected to produce increases in SSA and atmospheric DMS, as in the summer. SSA increases by 3.1% over the Southern Ocean, whereas DMS had negligible change (Figures 4d and 5e), coinciding with the general small increase in wind speeds (+0.28 m s^{-1}). G. Jones et al. (2020) previously identified a statistically significant negative relationship between oceanic DMS and wind speed with an r^2 value of 0.54. Our analysis displays a weak negative relationship which is not statistically significant (r^2 = 0.1; Figure 4) over the entire Southern Ocean. NorESM2-LM simulates a stronger negative correlation with oceanic DMS (r^2 = 0.5), consistent with the findings of G. Jones et al. (2020), whereas the other models have little to no correlation (r^2 = 0.02 and 0.033). Each model parameterization for oceanic DMS does not directly incorporate wind speed, but does so through other mechanisms (see Bock et al. (2021)).

Some areas show changes in DMS, SSA and AOD at 60°S which coincide with sea ice extent changes. A small region close to Antarctica, located within the contours in Figure 5, displays the region where we believe melting sea ice may have driven this increase. CMIP6 models show large areas of sea ice melt ≥10% located at the boundary of the sea ice extent (Figure 5a). Where areas of large sea ice melt occur, it is expected that marine aerosol fluxes will increase. Figure 5 shows the newly opened seawater promoting biogeochemical (Figure 5d)

and sea-to-air fluxes of DMS and SSA. From the period of 1950 onwards, the AOD within the melt zone has the highest temporal r^2 value (0.67) with the reduced sea ice concentration as a result of increased DMS and SSA concentrations in these regions, shown in Figure 5f in Supporting Information S1. Outside the melt zone, but remaining within the sea ice zone, AOD and sea ice have a poor temporal correlation ($r^2 = 0.18$), suggesting an enhancement of aerosol at these higher latitudes are a response to simulated sea ice melt, during spring. We note that although these changes are present in the CMIP6 historical simulations, they do not occur in observations. However, they do show that sea ice concentration changes may be an important driver of future aerosol loading change.

Most CMIP6 models have a negative Antarctic sea ice bias particularly during spring and summer with reasons for such biases differing for each model (Roach et al., 2020). For example, Yool et al. (2021) show that the UKESM1 sea ice bias maximizes during austral winter and spring, as a partial response to a warm bias in the Southern Ocean sea surface temperature (Sellar et al., 2019) which in turn can be related to issues in the simulation of cloud (Hyder et al., 2018). Thus, UKESM1 simulates a large increase in atmospheric DMS (up to 52%) where sea ice melt is prominent. Generally the simulated aerosol response to sea ice melt is as expected, with previous work in Brean et al. (2021) and Yan et al. (2020) identifying that marine phytoplankton and sea ice melt have significant roles in new particle formation and elevate H_2SO_4 and SSA over the Antarctic. Methane sulfonic acid (MSA) is an oxidation product of DMS, which would also be enhanced under these conditions, capable of growing existing aerosol particles and therefore impacting CDNC concentrations. MSA is included in five models where it is mainly used as an inert sink for sulfur; however only in NorESM2-LM does it directly impact aerosol formation.

Aerosol loading over the Southern Ocean (40°S–60°S) during the present-day in SON has increased relative to the period before ozone depletion by about 7% on average (Figure 5d). Thus, it appears that the indirect influence of ozone depletion on winds are more important in terms of changes in aerosol loading than the direct impact of shortwave radiation changes on DMS, and therefore sulfate aerosol. In addition, SSA has increased in greater concentration than DMS as a response to the increases to the winds, and as a result of sea ice melt.

4. Conclusions

Global model simulations provide the best and potentially only current way to understand how the behavior of aerosols may have changed since pre-industrial times in this region, as relevant observations for the pre-industrial period do not exist. Our results compare the present day with the pre-ozone hole era of 1940–1960 and therefore does not directly represent the changes which occurred from before 1940. Through the use of CMIP6 model output, we have shown that natural aerosol formation and loading have likely changed over the Southern Ocean as a result of anthropogenic activity.

We evaluated two pathways by which ozone depletion might influence marine aerosols over the Southern Ocean by analyzing historical simulations performed for CMIP6. We define direct impacts from ozone depletion as those linked with increased downward shortwave radiation impacting oceanic DMS production. Indirect influences are associated with perturbations in the surface westerly jet which influence marine aerosol emissions.

The summertime westerly wind strengthened between 1.14 and 1.8 m s^{-1} at 60°S, and weakened by up to 0.34 m s^{-1} near 40°S. The net influence on AOD over the Southern Ocean is an increase of 5.6% (averaged over 40–60 S), with a maxima of 23.9% at 60°S, suggesting that aerosol loading changes due to ozone depletion are primarily controlled by changes in surface winds. Increased wind speeds over the summertime Southern Ocean result in increases of 3.2% in SSA and 0.82% in atmospheric DMS on average. At 60°S, larger increases in SSA and DMS are seen, of 9.7% and 3%, respectively. As a consequence of Antarctic ozone depletion and its impact on wind-driven marine aerosol fluxes, the Southern Ocean can therefore not be considered to be representative of a pristine aerosol environment during summertime, as was suggested by Hamilton et al. (2014). Future studies using the Southern Ocean as a proxy for the pre-industrial aerosol environment should therefore account for the anthropogenic influence on aerosols during austral summer due to the ozone hole.

The direct influence of the ozone hole enhancing shortwave radiation does not have a discernible impact on oceanic DMS in spring, possibly because of the obscuring effect of changes in the tropospheric westerly jet which dominate. Oceanic and atmospheric DMS in spring is also strongly influenced by areas of sea ice reduction. Future Southern Ocean aerosol will not only be controlled by changes to the westerly jet, but as the Antarctic

sea ice melts, much greater volumes of aerosol could be produced (Brean et al., 2021; Yan et al., 2020). Given that the Antarctic ozone hole is showing early signs of recovery Solomon et al. (2016), future changes Southern Ocean aerosol loading via the westerly jet will also be influenced by ozone recovery and greenhouse gas forcing.

Data Availability Statement

CMIP6 model data used in this study are available from https://esgf-node.llnl.gov/search/cmip6/ for the UKESM1, BCC-ESM1, GFDL-CM4 and GFDL-ESM4, HadGEM3-GC3.1-LL, MRI-ESM2-0, NorESM2-LM, MPI-ESM-1-2-HAM and MIROC-ES2L. The respective raw data used in this study can be obtained from the above url with each model reference found in Table 1 and corresponding doi located below.

Acknowledgments
This research was supported by the Deep South National Science Challenge (Grant Nos. C01X141E2 and C01X1901). The authors acknowledge the World Climate Research Programme, which, through its Working Group on Coupled Modelling, coordinated and promoted CMIP6. We thank the climate modeling groups for producing and making available their model output, the Earth System Grid Federation (ESGF) for archiving the data and providing access, and the multiple funding agencies who support CMIP6 and ESGF. Open access publishing facilitated by University of Canterbury, as part of the Wiley - University of Canterbury agreement via the Council of Australian University Librarians.

References

Arrigo, K. R. (1994). Impact of ozone depletion on phytoplankton growth in the Southern Ocean: Large-scale spatial and temporal variability. *Marine Ecology Progress Series*, *114*, 1. https://doi.org/10.3354/meps114001

Banerjee, A., Fyfe, J. C., Polvani, L. M., Waugh, D., & Chang, K.-L. (2020). A pause in Southern Hemisphere circulation trends due to the Montreal Protocol. *Nature*, *579*(7800), 544–548. https://doi.org/10.1038/s41586-020-2120-4

Bell, T., De Bruyn, W., Marandino, C. A., Miller, S., Law, C., Smith, M., & Saltzman, E. (2015). Dimethylsulfide gas transfer coefficients from algal blooms in the southern ocean. *Atmospheric Chemistry and Physics*, *15*(4), 1783–1794. https://doi.org/10.5194/acp-15-1783-2015

Bell, T., De Bruyn, W., Miller, S., Ward, B., Christensen, K., & Saltzman, E. (2013). Air–sea dimethylsulfide (DMS) gas transfer in the North Atlantic: Evidence for limited interfacial gas exchange at high wind speed. *Atmospheric Chemistry and Physics*, *13*(21), 11073–11087. https://doi.org/10.5194/acp-13-11073-2013

Blomquist, B. W., Brumer, S. E., Fairall, C. W., Huebert, B. J., Zappa, C. J., Brooks, I. M., et al. (2017). Wind speed and sea state dependencies of air-sea gas transfer: Results from the high wind speed gas exchange study (HIWINGS). *Journal of Geophysical Research: Oceans*, *122*(10), 8034–8062. https://doi.org/10.1002/2017jc013181

Bock, J., Michou, M., Nabat, P., Abe, M., Mulcahy, J. P., Olivié, D. J., et al. (2021). Evaluation of ocean dimethylsulfide concentration and emission in CMIP6 models. *Biogeosciences*, *18*(12), 3823–3860. https://doi.org/10.5194/bg-18-3823-2021

Bracegirdle, T., Holmes, C., Hosking, J., Marshall, G., Osman, M., Patterson, M., & Rackow, T. (2020). Improvements in circumpolar southern hemisphere extratropical atmospheric circulation in CMIP6 compared to CMIP5. *Earth and Space Science*, *7*(6), e2019EA001065. https://doi.org/10.1029/2019ea001065

Bracegirdle, T. J., Krinner, G., Tonelli, M., Haumann, F. A., Naughten, K. A., Rackow, T., et al. (2020). Twenty first century changes in Antarctic and Southern Ocean surface climate in CMIP6. *Atmospheric Science Letters*, *21*(9), e984. https://doi.org/10.1002/asl.984

Brean, J., Dall'Osto, M., Simó, R., Shi, Z., Beddows, D. C., & Harrison, R. M. (2021). Open ocean and coastal new particle formation from sulfuric acid and amines around the Antarctic Peninsula. *Nature Geoscience*, *14*(6), 383–388. https://doi.org/10.1038/s41561-021-00751-y

Carslaw, K. S., Lee, L. A., Reddington, C. L., Pringle, K. J., Rap, A., Forster, P. M., et al. (2013). Large contribution of natural aerosols to uncertainty in indirect forcing. *Nature*, *503*(7474), 67–71. Retrieved from https://www.ncbi.nlm.nih.gov/pubmed/24201280

Cavalieri, D., Crawford, J., Drinkwater, M., Eppler, D., Farmer, L., Jentz, R., & Wackerman, C. (1991). Aircraft active and passive microwave validation of sea ice concentration from the defense meteorological satellite program special sensor microwave imager. *Journal of Geophysical Research*, *96*(C12), 21989–22008. https://doi.org/10.1029/91jc02335

Chiodo, G., Polvani, L. M., & Previdi, M. (2017). Large increase in incident shortwave radiation due to the ozone hole offset by high climatological albedo over Antarctica. *Journal of Climate*, *30*(13), 4883–4890. https://doi.org/10.1175/jcli-d-16-0842.1

Erickson, D. J., III., Zepp, R. G., & Atlas, E. (2000). Ozone depletion and the air–sea exchange of greenhouse and chemically reactive trace gases. *Chemosphere: Global Change Science*, *2*(2), 137–149. https://doi.org/10.1016/s1465-9972(00)00006-4

Eyring, V., Bony, S., Meehl, G. A., Senior, C. A., Stevens, B., Stouffer, R. J., & Taylor, K. E. (2016). Overview of the coupled model intercomparison project phase 6 (CMIP6) experimental design and organization. *Geoscientific Model Development*, *9*(5), 1937–1958. https://doi.org/10.5194/gmd-9-1937-2016

Farman, J. C., Gardiner, B. G., & Shanklin, J. D. (1985). Large losses of total ozone in Antarctica reveal seasonal CLO x/no x interaction. *Nature*, *315*(6016), 207–210. https://doi.org/10.1038/315207a0

Fossum, K. N., Ovadnevaite, J., Ceburnis, D., Dall'Osto, M., Marullo, S., Bellacicco, M., et al. (2018). Summertime primary and secondary contributions to southern ocean cloud condensation nuclei. *Scientific Reports*, *8*(1), 1–14. https://doi.org/10.1038/s41598-018-32047-4

Gillett, N. P., & Thompson, D. W. (2003). Simulation of recent southern hemisphere climate change. *Science*, *302*(5643), 273–275. https://doi.org/10.1126/science.1087440

Gong, S. L. (2003). A parameterization of sea-salt aerosol source function for sub- and super-micron particles. *Global Biogeochemical Cycles*, *17*(4). https://doi.org/10.1029/2003gb002079

Gonzalez, P. L., Polvani, L. M., Seager, R., & Correa, G. J. (2014). Stratospheric ozone depletion: A key driver of recent precipitation trends in South eastern South America. *Climate Dynamics*, *42*(7), 1775–1792. https://doi.org/10.1007/s00382-013-1777-x

Goyal, R., Sen Gupta, A., Jucker, M., & England, M. H. (2021). Historical and projected changes in the southern hemisphere surface westerlies. *Geophysical Research Letters*, *48*(4), e2020GL090849. https://doi.org/10.1029/2020gl090849

Grythe, H., Ström, J., Krejci, R., Quinn, P., & Stohl, A. (2014). A review of sea-spray aerosol source functions using a large global set of sea salt aerosol concentration measurements. *Atmospheric Chemistry and Physics*, *14*(3), 1277–1297. https://doi.org/10.5194/acp-14-1277-2014

Hamilton, D. S., Lee, L. A., Pringle, K. J., Reddington, C. L., Spracklen, D. V., & Carslaw, K. S. (2014). Occurrence of pristine aerosol environments on a polluted planet. *Proceedings of the National Academy of Sciences of the United States of America*, *111*(52), 18466–18471. https://doi.org/10.1073/pnas.1415440111

Hartery, S., Toohey, D., Revell, L., Sellegri, K., Kuma, P., Harvey, M., & McDonald, A. J. (2020). Constraining the surface flux of sea spray particles from the Southern Ocean. *Journal of Geophysical Research: Atmospheres*, *125*(4). https://doi.org/10.1029/2019jd032026

Hersbach, H., Bell, B., Berrisford, P., Hirahara, S., Horányi, A., Muñoz-Sabater, J., et al. (2020). The ERA5 global reanalysis. *Quarterly Journal of the Royal Meteorological Society*, *146*(730), 1999–2049. https://doi.org/10.1002/qj.3803

Ho, D. T., Law, C. S., Smith, M. J., Schlosser, P., Harvey, M., & Hill, P. (2006). Measurements of air-sea gas exchange at high wind speeds in the southern ocean: Implications for global parameterizations. *Geophysical Research Letters*, *33*(16), L16611. https://doi.org/10.1029/2006gl026817

Hoffmann, E. H., Tilgner, A., Schrödner, R., Bräuer, P., Wolke, R., & Herrmann, H. (2016). An advanced modeling study on the impacts and atmospheric implications of multiphase dimethyl sulfide chemistry. *Proceedings of the National Academy of Sciences*, *113*(42), 11776–11781. https://doi.org/10.1073/pnas.1606320113

Humphries, R. S., Keywood, M. D., Gribben, S., McRobert, I. M., Ward, J. P., Selleck, P., et al. (2021). Southern Ocean latitudinal gradients of cloud condensation nuclei. *Atmospheric Chemistry and Physics*, *21*(16), 12757–12782. https://doi.org/10.5194/acp-21-12757-2021

Hyder, P., Edwards, J. M., Allan, R. P., Hewitt, H. T., Bracegirdle, T. J., Gregory, J. M., et al. (2018). Critical Southern Ocean climate model biases traced to atmospheric model cloud errors. *Nature Communications*, *9*(1), 1–17. https://doi.org/10.1038/s41467-018-05634-2

Ivy, D. J., Solomon, S., & Rieder, H. E. (2016). Radiative and dynamical influences on polar stratospheric temperature trends. *Journal of Climate*, *29*(13), 4927–4938. https://doi.org/10.1175/jcli-d-15-0503.1

Jaeglé, L., Quinn, P. K., Bates, T. S., Alexander, B., & Lin, J. T. (2011). Global distribution of sea salt aerosols: New constraints from in situ and remote sensing observations. *Atmospheric Chemistry and Physics*, *11*(7), 3137–3157. https://doi.org/10.5194/acp-11-3137-2011

Jones, A. E., & Wolff, E. W. (2003). An analysis of the oxidation potential of the South Pole boundary layer and the influence of stratospheric ozone depletion. *Journal of Geophysical Research*, *108*(D18), 4565. https://doi.org/10.1029/2003jd003379

Jones, G., Harvey, M., King, S., Schneider, A., Wright, S., Fortescue, D., et al. (2020). Varying biological activity and wind stress affect the DMS response during the sage iron enrichment experiment. *Journal of Marine Science and Engineering*, *8*(4), 268. https://doi.org/10.3390/jmse8040268

Keeble, J., Hassler, B., Banerjee, A., Checa-Garcia, R., Chiodo, G., Davis, S., et al. (2021). Evaluating stratospheric ozone and water vapour changes in CMIP6 models from 1850 to 2100. *Atmospheric Chemistry and Physics*, *21*(6), 5015–5061. https://doi.org/10.5194/acp-21-5015-2021

Korhonen, H., Carslaw, K. S., Forster, P. M., Mikkonen, S., Gordon, N. D., & Kokkola, H. (2010). Aerosol climate feedback due to decadal increases in Southern Hemisphere wind speeds. *Geophysical Research Letters*, *37*(2). https://doi.org/10.1029/2009gl041320

Korhonen, H., Carslaw, K. S., Spracklen, D. V., Mann, G. W., & Woodhouse, M. T. (2008). Influence of oceanic dimethyl sulfide emissions on cloud condensation nuclei concentrations and seasonality over the remote southern hemisphere oceans: A global model study. *Journal of Geophysical Research*, *113*(D15), D15204. https://doi.org/10.1029/2007jd009718

Krall, K. E., Smith, A. W., Takagaki, N., & Jähne, B. (2019). Air–sea gas exchange at wind speeds up to 85 m s–1. *Ocean Science*, *15*(6), 1783–1799. https://doi.org/10.5194/os-15-1783-2019

Krasting, J. P., John, J. G., Blanton, C., McHugh, C., Nikonov, S., Radhakrishnan, A., et al. (2018). *NOAA-GFDL GFDL-ESM4 model output prepared for CMIP6 CMIP historical*. Earth System Grid Federation. https://doi.org/10.22033/ESGF/CMIP6.8597

Larsen, S. H. (2005). Solar variability, dimethyl sulphide, clouds, and climate. *Global Biogeochemical Cycles*, *19*(1). https://doi.org/10.1029/2004gb002333

Lin, P., Paynter, D., Polvani, L., Correa, G. J., Ming, Y., & Ramaswamy, V. (2017). Dependence of model-simulated response to ozone depletion on stratospheric polar vortex climatology. *Geophysical Research Letters*, *44*(12), 6391–6398. https://doi.org/10.1002/2017gl073862

Liss, P. S., & Merlivat, L. (1986). Air-sea gas exchange rates: Introduction and synthesis. In *The role of air-sea exchange in geochemical cycling* (pp. 113–127). Springer.

Llabrés, M., Agustí, S., Fernández, M., Canepa, A., Maurin, F., Vidal, F., et al. (2013). Impact of elevated UVB radiation on marine biota: A meta-analysis. *Global Ecology and Biogeography*, *22*(1), 131–144. https://doi.org/10.1111/j.1466-8238.2012.00784.x

Long, M. S., Keene, W. C., Kieber, D., Erickson, D., & Maring, H. (2011). A sea-state based source function for size-and composition-resolved marine aerosol production. *Atmospheric Chemistry and Physics*, *11*(3), 1203–1216. https://doi.org/10.5194/acp-11-1203-2011

Mahowald, N. M., Lamarque, J.-F., Tie, X. X., & Wolff, E. (2006). Sea-salt aerosol response to climate change: Last glacial maximum, preindustrial, and doubled carbon dioxide climates. *Journal of Geophysical Research*, *111*(D5), D05303. https://doi.org/10.1029/2005jd006459

McCoy, I. L., McCoy, D. T., Wood, R., Regayre, L., Watson-Parris, D., Grosvenor, D. P., et al. (2020). The hemispheric contrast in cloud microphysical properties constrains aerosol forcing. *Proceedings of the National Academy of Sciences of the United States of America*, *117*(32), 18998–19006. https://doi.org/10.1073/pnas.1922502117

Meinshausen, M., Nicholls, Z. R. J., Lewis, J., Gidden, M. J., Vogel, E., Freund, M., et al. (2020). The shared socio-economic pathway (SSP) greenhouse gas concentrations and their extensions to 2500. *Geoscientific Model Development*, *13*(8), 3571–3605. https://doi.org/10.5194/gmd-13-3571-2020

Mulcahy, J. P., Johnson, C., Jones, C. G., Povey, A. C., Scott, C. E., Sellar, A., et al. (2020). Description and evaluation of aerosol in UKESM1 and HadGEM3-GC3. 1 CMIP6 historical simulations. *Geoscientific Model Development*, *13*(12), 6383–6423. https://doi.org/10.5194/gmd-13-6383-2020

Neubauer, D., Ferrachat, S., Siegenthaler-Le Drian, C., Stoll, J., Folini, D., & Tegen, I. (2019). *Hammoz-consortium mpi-ESM1. 2-HAM model output prepared for CMIP6 aerchemmip*. Earth System Grid Federation. https://doi.org/10.22033/ESGF/CMIP6.1622

Nightingale, P. D., Malin, G., Law, C. S., Watson, A. J., Liss, P. S., Liddicoat, M. I., et al. (2000). In situ evaluation of air-sea gas exchange parameterizations using novel conservative and volatile tracers. *Global Biogeochemical Cycles*, *14*(1), 373–387. https://doi.org/10.1029/1999gb900091

Orr, A., Bracegirdle, T. J., Hosking, J. S., Jung, T., Haigh, J. D., Phillips, T., & Feng, W. (2012). Possible dynamical mechanisms for Southern Hemisphere climate change due to the ozone hole. *Journal of the Atmospheric Sciences*, *69*(10), 2917–2932. https://doi.org/10.1175/jas-d-11-0210.1

Peng, S., Liao, H., Zhou, T., & Peng, S. (2017). Effects of UVB radiation on freshwater biota: A meta-analysis. *Global Ecology and Biogeography*, *26*(4), 500–510. https://doi.org/10.1111/geb.12552

Revell, L., Robertson, F., Douglas, H., Morgenstern, O., & Frame, D. (2022). Influence of ozone forcing on 21st century southern hemisphere surface westerlies in CMIP6 models. *Geophysical Research Letters*, *49*(6), e2022GL098252. https://doi.org/10.1029/2022gl098252

Revell, L. E., Kremser, S., Hartery, S., Harvey, M., Mulcahy, J. P., Williams, J., et al. (2019). The sensitivity of Southern Ocean aerosols and cloud microphysics to sea spray and sulfate aerosol production in the HadGEM3-GA7. 1 chemistry–climate model. *Atmospheric Chemistry and Physics*, *19*(24), 15447–15466. https://doi.org/10.5194/acp-19-15447-2019

Revell, L. E., Wotherspoon, N., Jones, O., Bhatti, Y. A., Williams, J., Mackie, S., & Mulcahy, J. (2021). Atmosphere-ocean feedback from wind-driven sea spray aerosol production. *Geophysical Research Letters*, *48*(7), e2020GL091900. https://doi.org/10.1029/2020gl091900

Ridley, J., Menary, M., Kuhlbrodt, T., Andrews, M., & Andrews, T. (2019). *MOHC HadGEM3-GC31-LL model output prepared for CMIP6 CMIP historical*. Earth System Grid Federation. https://doi.org/10.22033/ESGF/CMIP6.6109

Roach, L. A., Dörr, J., Holmes, C. R., Massonnet, F., Blockley, E. W., Notz, D., et al. (2020). Antarctic sea ice area in CMIP6. *Geophysical Research Letters*, *47*(9), e2019GL086729. https://doi.org/10.1029/2019gl086729

Salter, M. E., Zieger, P., Acosta Navarro, J. C., Grythe, H., Kirkevåg, A., Rosati, B., et al. (2015). An empirically derived inorganic sea spray source function incorporating sea surface temperature. *Atmospheric Chemistry and Physics*, *15*(19), 11047–11066. https://doi.org/10.5194/acp-15-11047-2015

Schuddeboom, A. J., & McDonald, A. J. (2021). The southern ocean radiative bias, cloud compensating errors, and equilibrium climate sensitivity in CMIP6 models. *Journal of Geophysical Research: Atmospheres*, *126*(22), e2021JD035310. https://doi.org/10.1029/2021jd035310

Séférian, R., Berthet, S., Yool, A., Palmieri, J., Bopp, L., Tagliabue, A., et al. (2020). Tracking improvement in simulated marine biogeochemistry between CMIP5 and CMIP6. *Current Climate Change Reports*, *6*(3), 95–119. https://doi.org/10.1007/s40641-020-00160-0

Seland, Ø., Bentsen, M., Oliviè, D. J. L., Toniazzo, T., Gjermundsen, A., & Graff, L. S. (2019). *NCC NORESM2-LM model output prepared for CMIP6 CMIP historical* (Vol. 10). Earth System Grid Federation. https://doi.org/10.22033/ESGF/CMIP6.502

Sellar, A. A., Jones, C. G., Mulcahy, J. P., Tang, Y., Yool, A., Wiltshire, A., et al. (2019). UKESM1: Description and evaluation of the UK Earth system model. *Journal of Advances in Modeling Earth Systems*, *11*(12), 4513–4558. https://doi.org/10.1029/2019ms001739

Smith, R. C., Prezelin, B., Baker, K. e. a., Bidigare, R., Boucher, N., Coley, T., et al. (1992). Ozone depletion: Ultraviolet radiation and phytoplankton biology in Antarctic waters. *Science*, *255*(5047), 952–959. https://doi.org/10.1126/science.1546292

Sofiev, M., Soares, J., Prank, M., de Leeuw, G., & Kukkonen, J. (2011). A regional-to-global model of emission and transport of sea salt particles in the atmosphere. *Journal of Geophysical Research*, *116*(D21). https://doi.org/10.1029/2010jd014713

Solomon, S. (1999). Stratospheric ozone depletion: A review of concepts and history. *Reviews of Geophysics*, *37*(3), 275–316. https://doi.org/10.1029/1999rg900008

Solomon, S., Ivy, D. J., Kinnison, D., Mills, M. J., Neely, R. R., & Schmidt, A. (2016). Emergence of healing in the Antarctic ozone layer. *Science*, *353*(6296), 269–274. https://doi.org/10.1126/science.aae0061

Son, S.-W., Han, B.-R., Garfinkel, C. I., Kim, S.-Y., Park, R., Abraham, N. L., et al. (2018). Tropospheric jet response to Antarctic ozone depletion: An update with Chemistry-Climate Model Initiative (CCMI) models. *Environmental Research Letters*, *13*(5), 054024. https://doi.org/10.1088/1748-9326/aabf21

Son, S.-W., Tandon, N. F., Polvani, L. M., & Waugh, D. W. (2009). Ozone hole and Southern Hemisphere climate change. *Geophysical Research Letters*, *36*(15). https://doi.org/10.1029/2009GL038671

Swart, N. C., & Fyfe, J. C. (2012). Observed and simulated changes in the Southern Hemisphere surface westerly wind-stress. *Geophysical Research Letters*, *39*(16). https://doi.org/10.1029/2012gl052810

Swart, N. C., Fyfe, J. C., Gillett, N., & Marshall, G. J. (2015). Comparing trends in the southern annular mode and surface westerly jet. *Journal of Climate*, *28*(22), 8840–8859. https://doi.org/10.1175/jcli-d-15-0334.1

Tang, Y., Rumbold, S., Ellis, R., Kelley, D., Mulcahy, J., Sellar, A., et al. (2019). *MOHC UKESM1.0-LL model output prepared for CMIP6 CMIP historical*. Earth System Grid Federation. https://doi.org/10.22033/ESGF/CMIP6.6113

Tatebe, H., & Watanabe, M. (2018). *MIROC MIROC6 model output prepared for CMIP6 CMIP historical*. Earth System Grid Federation. https://doi.org/10.22033/ESGF/CMIP6.5603

Thompson, D. W., & Solomon, S. (2002). Interpretation of recent Southern Hemisphere climate change. *Science*, *296*(5569), 895–899. https://doi.org/10.1126/science.1069270

Thompson, D. W., Solomon, S., Kushner, P. J., England, M. H., Grise, K. M., & Karoly, D. J. (2011). Signatures of the Antarctic ozone hole in Southern Hemisphere surface climate change. *Nature Geoscience*, *4*(11), 741–749. https://doi.org/10.1038/ngeo1296

Vallina, S. M., Simó, R., & Gassó, S. (2006). What controls CCN seasonality in the Southern Ocean? A statistical analysis based on satellite-derived chlorophyll and CCN and model-estimated oh radical and rainfall. *Global Biogeochemical Cycles*, *20*(1). https://doi.org/10.1029/2005gb002597

Veres, P. R., Neuman, J. A., Bertram, T. H., Assaf, E., Wolfe, G. M., Williamson, C. J., et al. (2020). Global airborne sampling reveals a previously unobserved dimethyl sulfide oxidation mechanism in the marine atmosphere. *Proceedings of the National Academy of Sciences*, *117*(9), 4505–4510. https://doi.org/10.1073/pnas.1919344117

Wanninkhof, R. (1992). Relationship between wind speed and gas exchange over the ocean. *Journal of Geophysical Research*, *97*(C5), 7373–7382. https://doi.org/10.1029/92jc00188

Wanninkhof, R. (2014). Relationship between wind speed and gas exchange over the ocean revisited. *Limnology and Oceanography: Methods*, *12*(6), 351–362. https://doi.org/10.4319/lom.2014.12.351

Wu, T., Chu, M., Dong, M., Fang, Y., Jie, W., & Li, J. (2018). *BCC BCC-CSM2MR model output prepared for cmip6 cmip historical* (Vol. 10). Earth System Grid Federation. https://doi.org/10.22033/ESGF/CMIP6.1734

Yan, J., Jung, J., Lin, Q., Zhang, M., Xu, S., & Zhao, S. (2020). Effect of sea ice retreat on marine aerosol emissions in the Southern Ocean, Antarctica. *Science of the Total Environment*, *745*, 140773. https://doi.org/10.1016/j.scitotenv.2020.140773

Yang, G.-P., Zhang, H.-H., Zhou, L.-M., & Yang, J. (2011). Temporal and spatial variations of dimethylsulfide (DMS) and dimethylsulfoniopropionate (DMSP) in the East China Sea and the yellow sea. *Continental Shelf Research*, *31*(13), 1325–1335. https://doi.org/10.1016/j.csr.2011.05.001

Yool, A., Palmiéri, J., Jones, C., Sellar, A., de Mora, L., Kuhlbrodt, T., et al. (2020). Spin-up of UK Earth system Model 1 (UKESM1) for CMIP6. *Journal of Advances in Modeling Earth Systems*, *12*(8), e2019MS001933. https://doi.org/10.1029/2019ms001933

Yool, A., Palmiéri, J., Jones, C. G., de Mora, L., Kuhlbrodt, T., Popova, E. E., et al. (2021). Evaluating the physical and biogeochemical state of the global ocean component of UKESM1 in CMIP6 historical simulations. *Geoscientific Model Development*, *14*(6), 3437–3472. https://doi.org/10.5194/gmd-14-3437-2021

Yool, A., Popova, E. E., & Anderson, T. R. (2013). MEDUSA-2.0: An intermediate complexity biogeochemical model of the marine carbon cycle for climate change and ocean acidification studies. *Geoscientific Model Development*, *6*(5), 1767–1811. https://doi.org/10.5194/gmd-6-1767-2013

Yukimoto, S., Koshiro, T., Kawai, H., Oshima, N., Yoshida, K., Urakawa, S., et al. (2019). *MRI MRI-ESM2.0 model output prepared for CMIP6 CMIP historical*. Earth System Grid Federation. https://doi.org/10.22033/ESGF/CMIP6.6842

Zepp, R., Erickson, D., III, Paul, N., & Sulzberger, B. (2007). Interactive effects of solar UV radiation and climate change on biogeochemical cycling. *Photochemical and Photobiological Sciences*, *6*(3), 286–300. https://doi.org/10.1039/b700021a